SOLAR-REFLECTED RADIATION FROM THE SEA SURFACE

Dr. Robert E. Turner
Science Applications International Corporation
550 Camino El Estero, Suite 205
Monterey, CA 93940

Dr. Andreas K. Goroch
Naval Research Laboratory Monterey
7 Grace Hopper Avenue
Monterey, CA 93943-5506

ABSTRACT

For investigations in aircraft remote sensing and in the description of tactical decision aids for military operations it is usually assumed that solar radiation is of little significance in the thermal infrared portion of the electromagnetic spectrum. For many situations in atmospheric radiation models this is true because the Earth's surface consists of materials with diffuse or nearly diffuse reflectance properties. This is certainly not true, however, for water bodies as the surface is then specular or nearly specular, depending upon wind conditions. As a result, the ocean can reflect a large amount of radiation into an infrared sensor, thereby greatly reducing the effectiveness of that system. In this paper we present the results of computations of the directly-reflected solar radiation from a smooth ocean surface in terms of sun angle, atmospheric optical thickness, and wavelength. The importance of the solar effect is clearly indicated in various plots. As a result of this work it is clear that one can no longer neglect the effect of direct solar radiation in the thermal infrared part of the spectrum, especially for atmospheric radiation models which use infrared sensors in ocean operations.

1. INTRODUCTION

The extraterrestrial solar irradiance has a peak value in the visible part of the spectrum between 0.46 and 0.48 μm wavelength with only about 0.4 % of the solar radiation lying in the region beyond 5 pm. On the other hand, a *20° C* blackbody has a peak near 10 μm. It is interesting to compare the solar irradiance at the Earth's surface (with no atmospheric attenuation) and the irradiance of the blackbody at this wavelength. Thus,

Solar irradiance (5770 K) = 0.2858 Watts m‘2 μm^{-1}
Blackbody irradiance (20° C)= 28 Watts m‘2 μm^{-1}

It is apparent that the irradiance from the blackbody is about 100 times the solar value for a thermal infrared wavelength of 10 pm. The radiances (- irradiances/solid angle), however, are totally different, i.e.,

Solar radiance = 4205 Watts m‘2 sr^{-1} pm”
Blackbody radiance =9 Watts m^{-2} sr^{-1} pm-l

with a very large solar value as a result Of the small solid angle of the Sun. It is primarily for this reason that the radiation reflected from a nearly specular surface such as the ocean is so important in the thermal infrared part of the spectrum.

2. RADIOMETRIC QUANTITIES

The radiance reflected from a surface with bistatic reflectivity $r(\hat{\Omega}, \hat{\Omega}')$ is given by

$$L(\hat{\Omega}) = \int_{2\pi} r(\hat{\Omega}, \hat{\Omega}') L_{in}(\hat{\Omega}') d\hat{\Omega}' \tag{1}$$

for any arbitrary input radiation field integrated over the upper hemisphere. The “total” radiance from a general surface with a unidirectional solar input is given by

$$L(\hat{\Omega}) = E_0 r(\hat{\Omega}, \hat{\Omega}_0) T + \int_{2X} r(\hat{\Omega}, \hat{\Omega}') L_{sky}(\hat{\Omega}') d\hat{\Omega}' + \varepsilon_{eff}(\hat{\Omega}) B \tag{2}$$

where E_0 is the extraterrestrial solar irradiance at the top of Earth’s atmosphere, T is the transmittance through the atmosphere and B is the thermal radiance from a surface with an effective emissivity $\varepsilon_{eff}(\hat{\Omega})$. The second term in equation (2) is the contribution due to the integrated sky radiation. The corresponding radiance from a specular surface with a finite solid angle for the Sun is

$$L(\hat{\Omega}) = \frac{E_0 T \rho_F(\hat{\Omega}_0)}{\Omega_0} + \rho_F(\hat{\Omega}_0) L_{sky}(\hat{\Omega}_0) + \varepsilon(\hat{\Omega}_0) B \tag{3}$$

in the direction of the Sun with a Fresnel reflectance of $\rho_F(\hat{\Omega})$. Thus, in the limit, as a rough surface approaches a smooth surface the bistatic reflectivity becomes the Fresnel reflectance multiplied by the Dirac delta function for a unidirectional source. In this equation the emissivity is equal to one minus the Fresnel reflectance, whereas the effective emissivity in equation 2 is not equal to the one minus the bistatic reflectivity. Therefore, the solar radiances for a “point” Sun and for the actual Sun with a finite solid angle are given by

$$L_{Sun}(\hat{\Omega}) = E_0 \delta(\hat{\Omega} - \hat{\Omega}_0) \qquad \text{Infinite for a “point” Sun} \tag{4}$$

$$L_{Sun}(\hat{\Omega}) = \frac{E_0}{\Omega_{eff}} = \mathbf{4205}\ \text{Watts m‘2 sr’1 } \mu m^{-1} \qquad \text{Actual Sun} \tag{5}$$

where the numerical value for the finite Sun is for a wavelength of 10 μm with an effective photospheric temperature of 5770 K.

3. BISTATIC REFLECTANCE MODEL

The model for the sea surface that will be used is one developed by Yoshimori et al. [1,2,3,4] in a series of papers produced in recent years to characterize the wave structure of a wind-roughened water surface. A critical parameter in their model is the slope variance of the water waves, defined as

$$\gamma^2 = \int_0^\infty \Psi(\omega)[k(\omega)]^2 d\omega \qquad (6)$$

where $\Psi(\omega)$ is the so-called Joint North Sea Wave Project (JONS WAP) spectrum for water waves as described by Hasselmann et al. [5]. The quantity $k(\omega)$ is the wave propagation constant which is related to the angular frequency by the dispersion relation

$$\omega(k) = \left[\left(\frac{g}{k} + \frac{\Gamma k}{\rho}\right)\tanh(hk)\right]^{1/2} k \qquad (7)$$

where g(= 9.80665 m S^{-2}) is the acceleration due to gravity, Γ (=0.07353 N m^{-1}) is the surface tension, ρ (= 1024.75 kg m^{-3}) is the water density, and h(= 100 m) is the water depth. In addition, we will assume a water salinity of 35 parts per thousand and a surface water temperature of 20° Celsius. The JONSWAP spectrum is depicted in Fig. 1 for three wind speeds

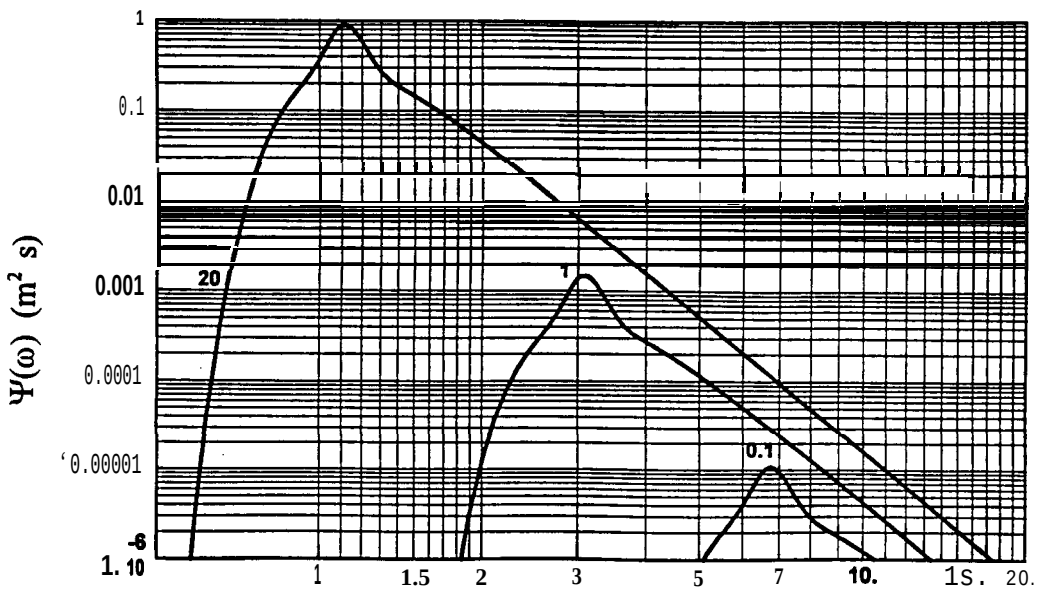

Fig. 1. JONSWAP spectrum for various wave speeds (m S-l) for a fetch of 40 km.

and for a fetch (range for which the wind blows uniformly over the surface) of 40 kilometers. Likewise, Fig. 2 illustrates the dependence of the square root of the slope variance (y) on the wind speed. It should be noted that this quantity is very sensitive to the wind speed for low values between zero and -1 meter per second.

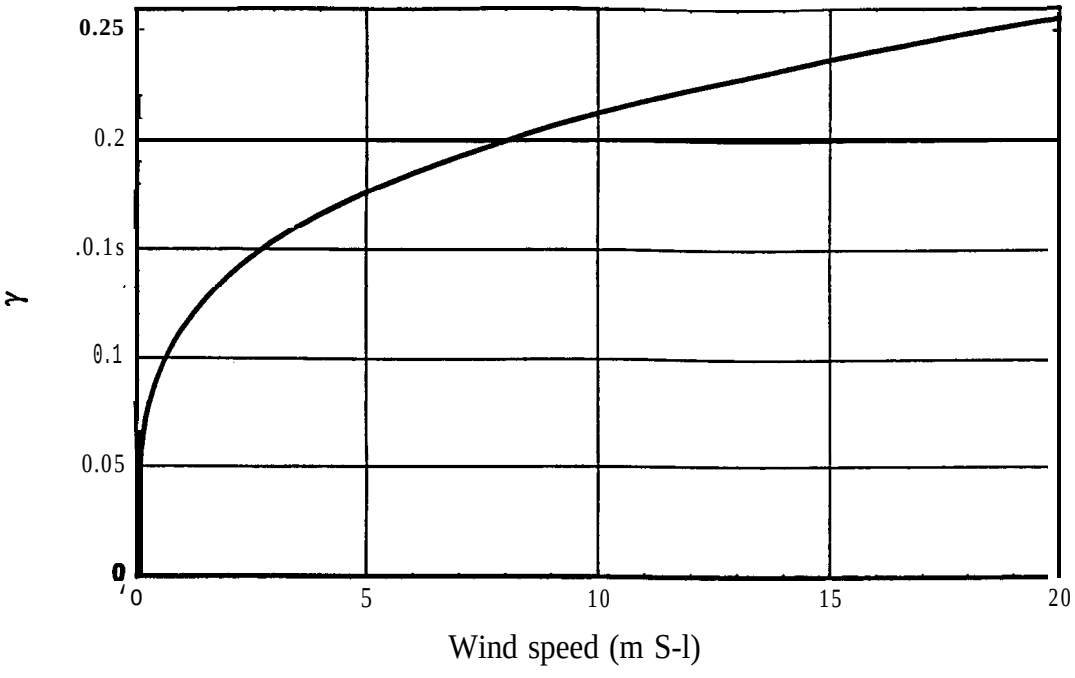

Fig. 2. Square root of the wave slope variance vs. wind speed (m S-l).

Using Gaussian distributions for the wave slopes in both the x and y directions on a horizontal surface, Yoshimori et al. [4] developed a closed-form expression for the bistatic reflectivity of the water surface for a point source of radiation. On the other hand, Zeisse [6] developed a formulation to account for a finite solid angle source. We have used these formulas to compute the bistatic reflectivity for water at a wavelength of 10 μm with a complex index of refraction of 1.210-0.055 i for the particular case when the solar zenith angle is equal to the nadir view angle of 85 degrees. The results are illustrated in Fig. 3. The agreement is excellent for wind speeds from 20 m s^{-1} down to about 0.1 m S-* but as the wind speed decreases to zero there is a discrepancy as the "delta-fiction" approximation increases without bound. The exact value for a wind speed of zero is known for the "finite Sun" case however, since it is the Fresnel reflectance divided by the solid angle of the Sun, i.e.,

$$r(\hat{\Omega},\hat{\Omega}_0) = \rho_F(\hat{\Omega}_0) / \Omega_0 = 7707 \text{ sr}^{-1} \qquad \text{Finite Sun} \qquad (8)$$

The exact calculation was performed down to a wind speed of 0.01 m s^{-1} but computations for lower wind speeds were discontinued because of the excessive computer time required. Nevertheless$, the plot does clearly show that the delta-fiction, closed-form method of Yoshimori et al. [4] is valid throughout a broad range of wind speeds.

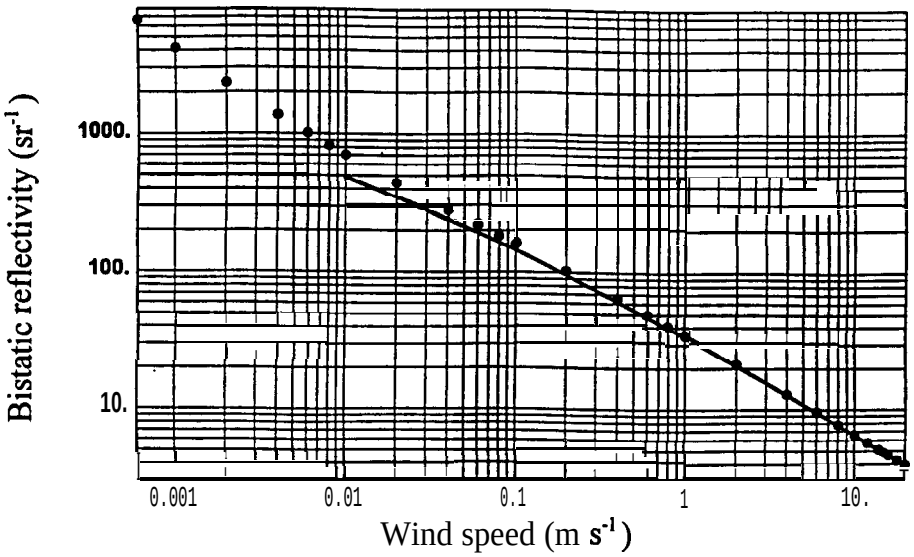

Fig. **3.** Comparison between the delta-fiction method of Yoshimori et al. (points) and the exact formula (solid line) for the **bistatic** reflectivity. Solar zenith angle is equal **to the** nadir view angle = 85°.

4. RADIATION COMPUTATIONS

In a manner similar to that for the **bistatic** reflectivity, Yoshimori et al. [4] also developed a formulation for the effective **emissivity** of a water surface by integrating the **Fresnel** reflectance over the distribution of wave slopes. Because **emissivity only** depends upon the outgoing direction the formulation **is** not as complicated as for the bistatic reflectivity. Multiplying the effective **emissivity** by the **Planck** radiance for a **blackbody** at a temperature of 20° C allows us to compute the thermal radiance from the water surface. **It** is depicted in **Fig.** 4 as a **function** of the wind speed for the large nadir view angle region from 70° to 90°. As the **viewer** looks straight down at the surface the radiance is about **8** Watts m^{-2} sr'* μm^{-1} but for large nadir angles there is significant departure in terms of the wind speed. It should be noted that the viewer is assumed to beat or near the surface so that atmospheric attenuation can be neglected.

The more interesting situation is for the bistatic reflectivity as a **function** of the incident Sun angle and the wind speed, U expressed in m S-*. Figure 5 illustrates the variation of the sum of the reflected radiance and the emitted radiance in terms of wind speed for a large nadir view angle of 89°. In all cases the **extraterrestrial** solar irradiance is 0.2858 Watts m^{-2} μm^{-1} and the attenuation of the incoming solar radiation has been computed using the computer program MODTRAN 3 [7]. We have chosen the U. S. Standard atmosphere with the Navy maritime model and an air-mass parameter of 5 which means that the observer is somewhere between the coast and the open sea. One can see that the radiance is not much greater than the "background" value of the emitted radiance for these wind speeds, but if we use lower wind speeds such as those in Fig. 6, the total radiance is considerable greater than the emitted radiance. We can also examine the **radiance** as a function of the nadir view angle and wind speed. Calculations were made for various Sun angles and the largest effect seems to be for a solar zenith angle of 83°.

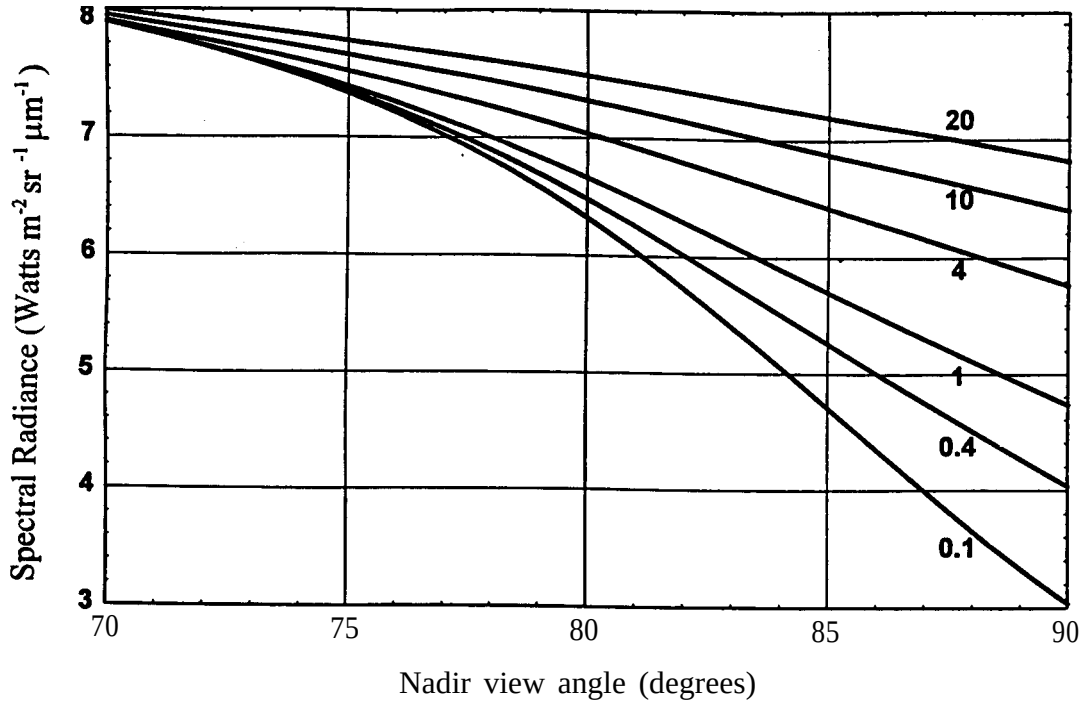

Fig. 4. Thermal spectral radiance vs. nadir view angle for water waves with various wind speeds (m S-l).

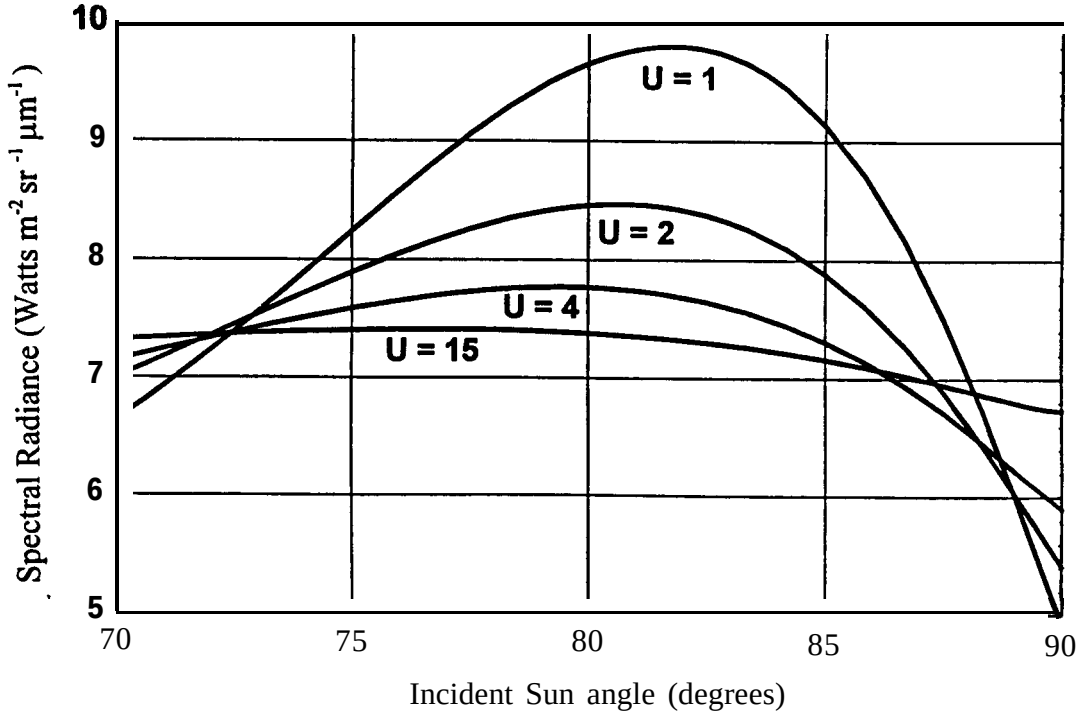

Fig. 5. Total spectral radiance vs. solar zenith angle for water waves with various high wind speeds (m s^{-1}) and a nadir view angle of 89° with the atmospheric attenuation computed according to the program MODTRAN 3.

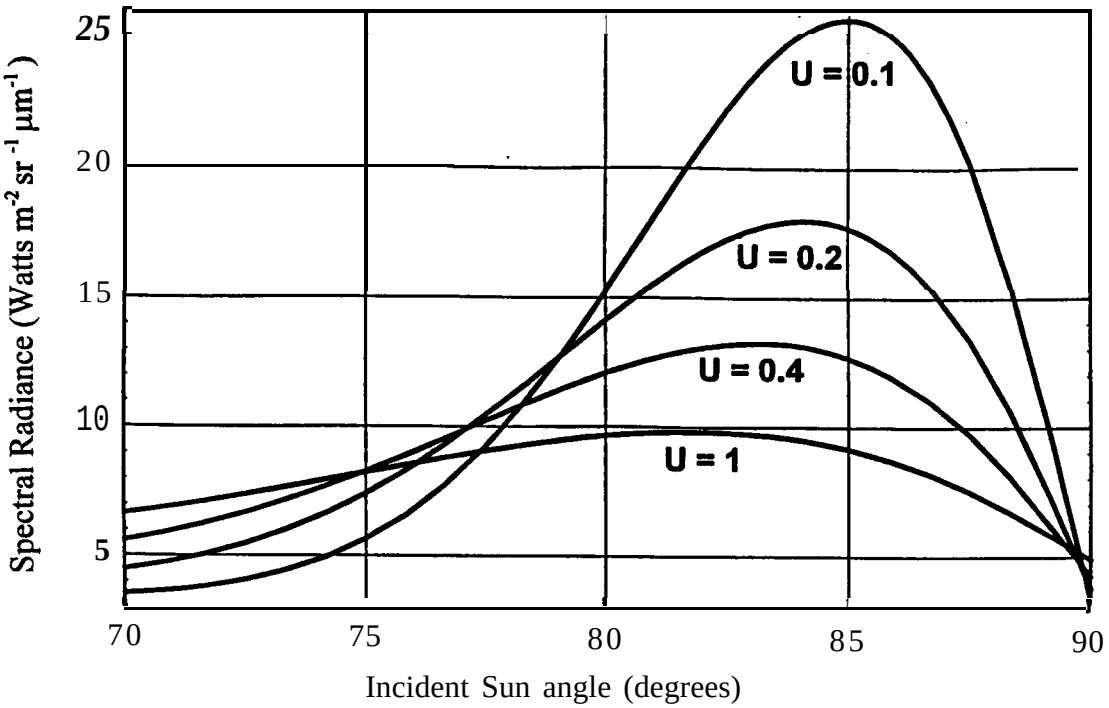

Fig. 6. Total spectral radiance vs. solar zenith angle for water waves with various low wind speeds (m S-l) and a nadir view angle of 89° with the atmospheric attenuation computed according to the program MODTRAN 3.

The variation is illustrated in Fig. 7 for four wind speeds where it is important to realize that the total radiance here is much greater than the thermal background for wind speeds below about 0.2 m S-l. The most important feature to be noticed, however, is the variation in the radiance from the surface facets in terms of the nadir view angle. Figure 8 depicts this interesting result of the total radiance for four facet slopes. The curves here are those for the reflected and emitted radiance for Fresnel reflectors taking into consideration the atmospheric attenuation, which accounts for the sharp decrease on the right side of each curve. The radiance values can be at least forty times greater than the thermal background values, a fact that is not always understood for the infrared part of the spectrum.

The radiation components can also be calculated explicitly in terms of the wind speed for various nadir view angles and solar zenith angles. Fig. 9 illustrates the variability in the thermal radiance with wind speed for three nadir view angles. For these large angles the thermal radiation is quite small for low wind speeds because the surface is nearly specular whereas this is not true for the rough surface generated by the high wind speeds. In Fig. 10 the total radiance is illustrated as a function of the wind speed from 1 ms'1 to 20 m S-l for the same three angles. Below one m S-l all radiances increase up to the Fresnel limit for zero wind speed but as the wind speed increases the radiance decreases to a minimum value because of the increasing surface roughness. Eventually, however, the total radiance increases again because of the thermal background.

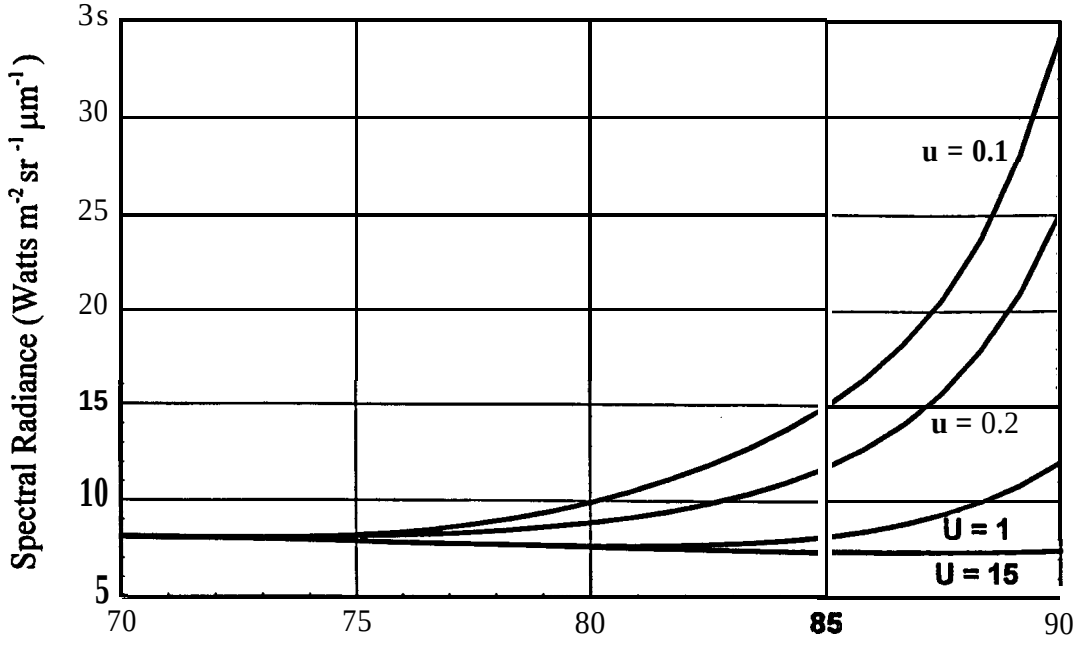

Fig. 7. Spectral radiance vs. nadir view angle for water waves with various wind speeds ($m\ s^{-1}$) and a solar zenith angleof830.

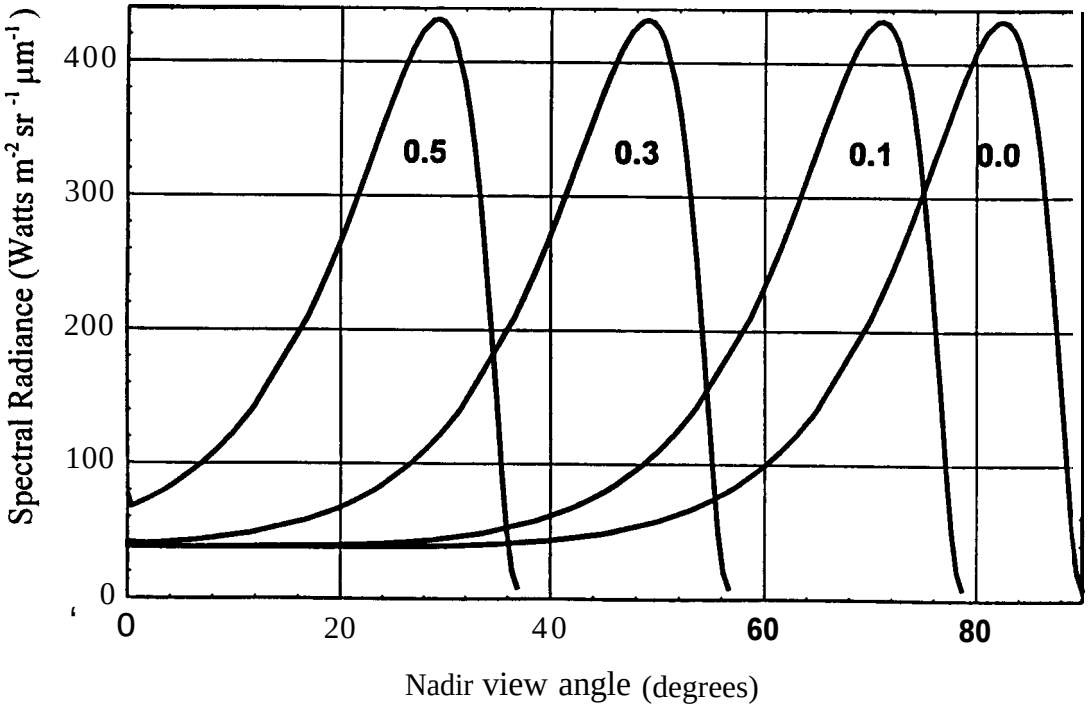

Fig. *8.* Spectral radiance vs. nadir view angle for water waves with various instantaneous slopes.

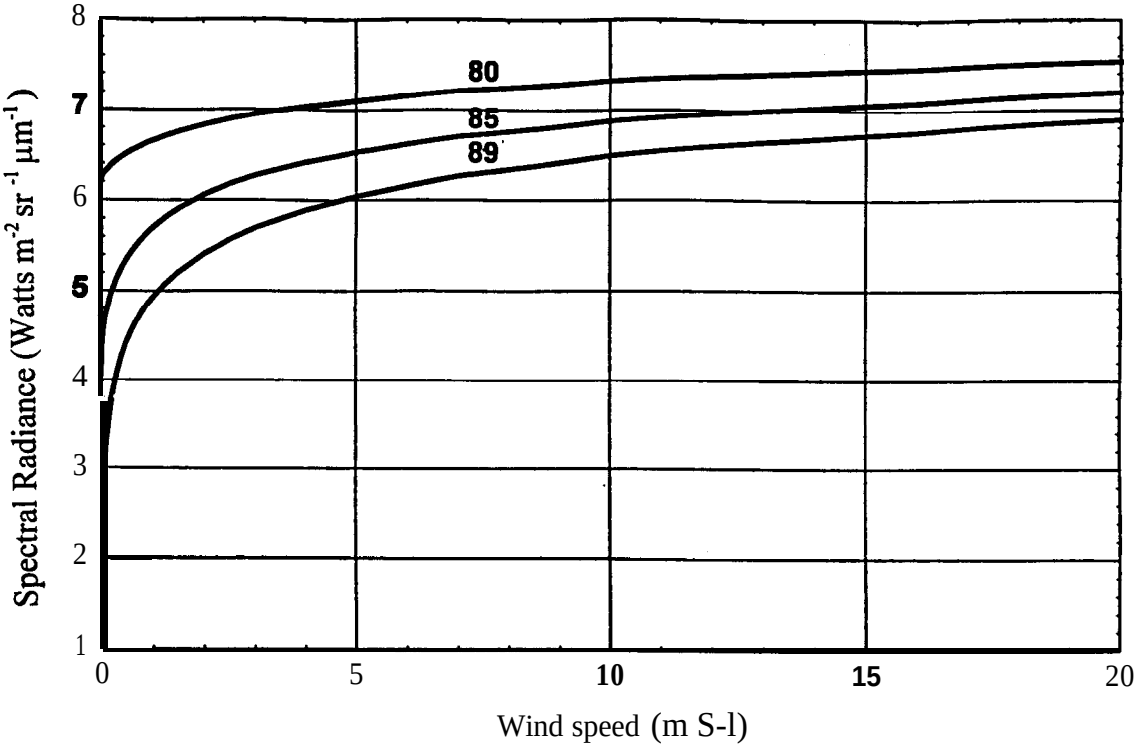

Fig. 9. Thermal spectral radiance vs. windspeed forwater waves for three nadir view angles (degrees).

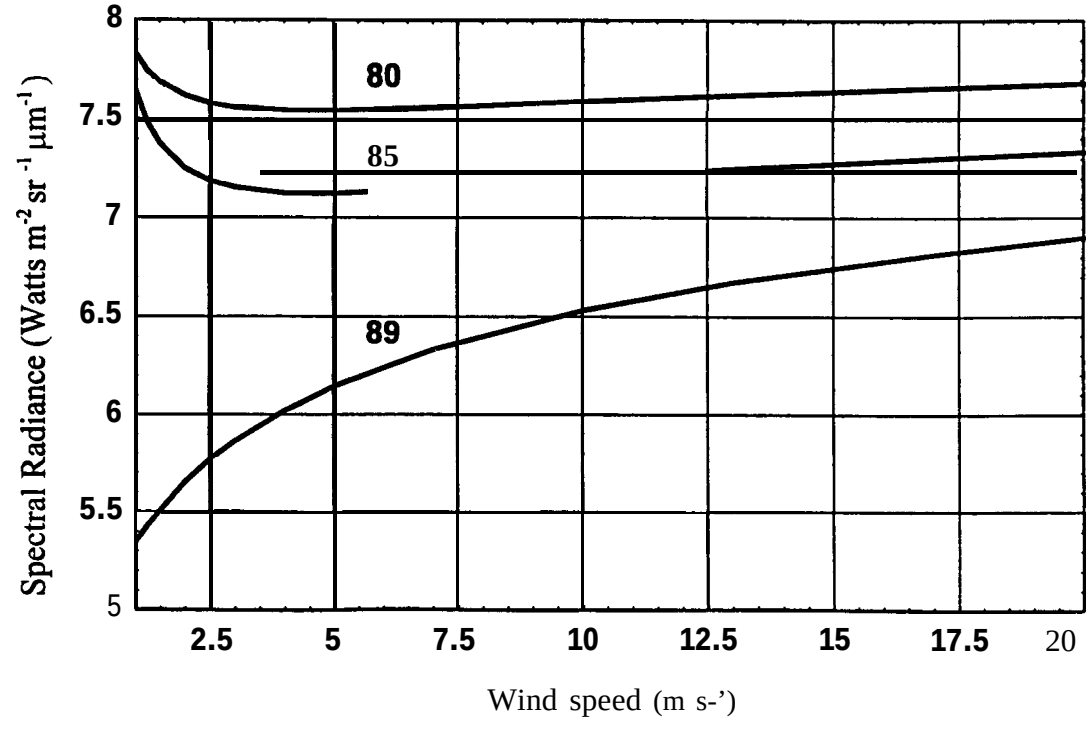

Fig. 10. Total spectral radiance vs. wind speed for water waves for three solar zenith angles (= nadir view angles) with the atmospheric attenuation computed according to the program MODTRAN 3.

5. CONCLUSIONS

It has clearly been demonstrated that the average solar-reflected radiance from a water surface in the thermal infrared part of the spectrum (~ 10 μm) can, under certain circumstances, be quite large, in a manner not unlike the similar well-known result in the visible part of the spectrum. The effect is especially significant for low wind speeds and for large nadir view angles. In addition, the infrared speckle pattern should be quite noticeable as can be seen from the large instantaneous reflected radiances from the individual facets with slopes from zero to 0.5. The hemispherical sky radiance has not been included in the present calculations but it has been estimated to be relatively small. Nevertheless, for completeness it should be included in the calculations although it is dependent upon the particular atmospheric model. Also, it would be instructive to calculate these effects for other wavelengths, fetch lengths, and atmospheres.

REFERENCES

1. K. Yoshimori, K. Itoh, and Y. Ichioka, "Statistical formulation for an inhomogeneous random water surface: a basis for optical remote sensing of oceans," J. Opt. Sot. Am. A, Vol. 11, No. 2,723-730 (1994).

2. K. Yoshimori, K. Itoh, and Y. Ichioka, " Thermal radiative and reflective characteristics of a wind-roughened water surface," J. Opt. Sot. Am. A, Vol. 11, No. 6, 1886-1893 (1994).

3. K. Yoshimori, K. Itoh, and Y. Ichioka, "Statistically corrected ocean thermography," Applied Optics, Vol. 33, No. 30,7078-7087, (1994).

4. K. Yoshimori, K. Itoh, and Y. Ichioka, "Optical characteristics of a wind-roughened water surface: a two-dimensional theory," Applied Optics, Vol. 34, No. 27,6236-6247, (1995).

5. K. Hasselmann, T. P. Barnett, E. Bouws, H. Carlson, D. E. Cartwright, K. Enke, J. A. Ewing, H. Gienapp, D. E. Hasselmann, P. Kruseman, A. Meerburg, P. Muller, D. J. Olbers, K. Richter, W. Sell, and H. Walden, ***Measurements of Wind- Wave Growth and Swell Decay during the Joint North Sea Wave Project (JONSWAP),*** (Deutsches Hydrographisches Institut, Hamburg, Germany, 1973).

6. C. R. Zeisse, "Radiance of the ocean horizon," J. Opt. Sot. Am. A, Vol. 12, No. 9,2022-2030, (1995).

7. MODTRAN 3, A Moderate Resolution Model of LOWTRAN 7, A. Berk, L. S. Bernstein, and D. C. Robertson, Spectral Sciences, Inc., Burlington, Final Report, GL-TR-889-0 122, 30 April 1989.